RSC Advances




ROYAL SOCIETY OF CHEMISTRY

www.rsc.org/advances

Journal Name

ARTICLE

# Intramolecular energy transfer dynamics in differently linked Zinc porphyrin-dithiaporphyrin dyads

Received 00th January 20xx,
Accepted 00th January 20xx

DOI: 10.1039/x0xx00000x

www.rsc.org/

**R.Ghosh[a], M. Yedukondalu,[b]M. Ravikanth,[b]and D. K.Palit[a*]**

Intramocular energy transfer dynamics in two molecular dyads, in which Zinc porphyrin ($ZnN_4$) and dithiaporphyrin ($N_2S_2$) units have been linked covalently by different bridges, namely phenylene (*ph*) and diphenylethyne (*dpe*), studied employing ultrafast time-resolved transient absorption and fluorescence spectroscopic techniques. The rates of energy transfer in both these dyads are slower than the corresponding $ZnN_4 – N_4$ dyads, in spite of better gradient for energy flow in the case of $ZnN_4 – N_2S_2$ dyads. Quantum chemical calculations reveal that the frontier orbital characteristics of the porphyrins is not significantly altered by sulphur substitution at the acceptor porphyrin core, thus does not modify the electronic factor in the energy transfer mechanism. However, significant decrease in overlap between the absorption spectrum of the donor and emission spectrum of the acceptor results in lower efficiency of the intramolecular energy transfer. Energy transfer process in dpe - linked dyads follows through-bond super-exchange mechanism, whereas, in ph - linked dyads, the through-space multipole resonance interaction plays important role.

## Introduction

Studies on energy transfer dynamics in multi-chromophoric arrays have long been devoted to mimic natural photosynthetic light harvesting mechanism and to develop artificial photosynthetic systems.[1-3]Understanding the rates and mechanisms of energy flow in multi-chromophoric arrays is essential for the rational design of molecular architectures with superior light-harvesting performance. Multi-porphyrin assemblies have gained special interest due to their role as energy surrogates for the natural photosynthetic antenna complexes. A large number of such arrays have been synthesized by covalent as well as noncovalent approaches and excited state properties were examined with regards to their energy-transfer properties.[4-19]In recent time, covalently linked multi-porphyrin arrays have been extensively explored to understand not only the light-harvesting properties but also the energy flow mechanism. To this end, several covalently linked metalloporphyrin-porphyrin dyads with different linkers and linker positions have been systematically synthesized and employed for the mechanistic studies of energy transfer.[9-16]In all these studies, free base porphyrin has been used as energy trap, whereas various metalloporphyrins and linking architecture as the light collection and energy donor unit. Through-bond Dexter mechanism has been deciphered to be the governing factor determining the energy transfer rate in covalently bonded multi-porphyrin assemblies. Frontier orbital characteristics have been revealed as a crucial factor to decide the rate of energy transfer.[13, 14]A common feature among the various multi-porphyrin arrays reported in the literature is that they invariably contain free base porphyrincore ($N_4$) as the energy acceptor unit. The energy transfer properties of such symmetrical porphyrin arrays containing $N_4$porphyrin cores have been studied by creating an energy gradient between the two or more porphyrin subunits by insertion of a metal such as Zn(II), Mg(II), orCd(II) in one of the porphyrin subunits and leaving the other porphyrin subunit in the free base form.

In recent past, synthesis of hetero-porphyrin derivatives have been of great interest because of significant variation of chemical and photophysical properties on core modification.[20-24]Hetero-porphyrins are prepared by modification of the porphyrin core by replacing one or two nitrogen atoms by another hetero-atom, like oxygen, sulphur etc. These core-modified porphyrins possess significantly lower singlet state energy than that of the free base porphyrin. This creates a suitable energy gradient in the excited singlet state for efficient energy flow from the metalloporphyrin to freebase porphyrin. This property can make them suitable for construction of artificial light harvesting systems. A large number of dyads containing hetero-porphyrins have been synthesized to study the energy transfer properties.[25-30]Although, steady state studies have revealed efficient energy transfer process, detailed mechanism of the energy transfer dynamics has not been explored because the energy transfer rates in these dyads have not been reported from time resolved studies having high temporal resolution. In this paper, we describe the energy transfer dynamics in a pair of

[a] *Radiation and Photochemistry Division, Bhabha Atomic Research centre, Mumbai-400085, India.*
[b] *Department of Chemistry, Indian Institute of Technology, Mumbai-400076, India.*

porphyrin dyads, in which zinc tetraphenylporphyrin($ZnN_4$) and dithiaporphyrin ($N_2S_2$)have been linked by two different linker groups, namely, diphenylethynyl and phenyl linker (Scheme I). We have employed sub-picosecond transient absorption and picosecond fluorescence spectroscopic techniques to determine the energy transfer rates in these two dyads and to compare them with those of the free base porphyrin analogues reported earlier. Differences in the rates of energy transfer between these two classes of porphyrin dyads have been rationalized and mechanistic aspects have been enumerated from the comparison of the frontier molecular orbital characteristics of porphyrin and dithiaporphyrin.

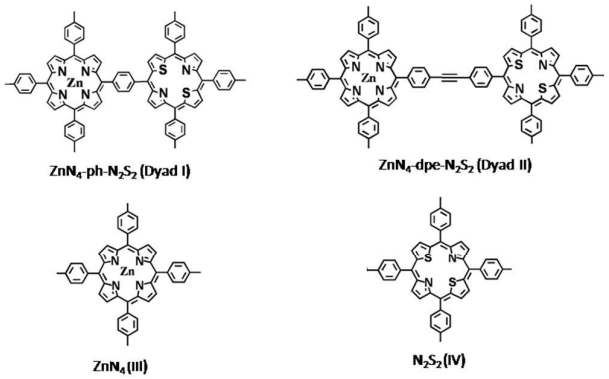


**Scheme I.** Structures of the two hetero-porphyrindyadsand corresponding sub-units used in the present study.

## Experimental methods

Detailed methods of synthesis of two hetero-porphyrin dyads, namely, $ZnN_4$-Ph-$N_2S_2$ (Dyad I) and $ZnN_4$-dpe-$N_2S_2$ (Dyad II) as well as the corresponding sub-units, namely, $ZnN_4$ (III) and $N_2S_2$ (IV) (Scheme I), have been reported earlier.[27, 28] Toluene of spectroscopic grade (Spectrochem, India) was used as received without further purification in all the spectroscopic measurements. Toluene was chosen because it is a non-coordinating and non-interacting solvent and readily solubilizes porphryin dyads up to desired concentrations required for time resolved experiments. Steady state absorption and fluorescence spectra were recorded with Thermo Spectronic (Biomate-5) absorption spectrometer and Varian (Cary Eclipse) spectrofluorimeter, respectively. Fluorescence spectra were corrected for the wavelength dependence of the instrument sensitivity.

Dynamics of the excited states were monitored following photoexcitation using 400 nm laser pulses by using a femtosecond pump−probe transient absorption spectrometer, which has been described in detail elsewhere.[31] The pulses of 50 fs duration and 200 μJ/pulse energy at 800 nmat1 kHz repetition rate were obtained from an amplified laser system (Thales, France). Pump pulses at 400 nm (energy ~ 5 μJ/pulse) were generated by frequency-doubling of one part of the 800 nm output of the amplifier in a 0.5 mm thick BBO crystal and a small amount from the other part (energy ~1μJ/pulse) to generate the white light continuum (480 - 1000 nm) probe in a 2 mm thick sapphire plate. The polarization of the pump beam was fixed at the magic angle with respect to that of the probe beam. The sample solutions were flown through a quartz cell of 1 mm path length during measurement. Decay dynamics at a particular wavelength region (10 nm width)was selected using a pair of interference filters placed in front of the photodiodes.The overall time resolution of the absorption spectrometer is about 120 fs. The temporal profiles recorded in the 480−750 nm wavelength region were fitted up to three exponentially rising or decaying components by iterative deconvolution method using an $sech^2$ type instrument response function with full width at half-maximum of 120 fs and were also used for constructing the time-resolved differential absorption spectra. All the experiments were performed at 296K.

Picosecond time resolved fluorescence studies were performed using a streak camera detector (Optoscope-SC10, Optronis, Germany).Samples were excited using 400 nm laser pulses of 50 fs duration obtained from the laser system described above. Fluorescence from the sample was collected (perpendicular to excitation) and focused to input slit of a spectrograph (Spectral Product, DK240), which spectrally disperses the fluorescence signal and produces a vertical image at the spectrograph output. Spectrally dispersed fluorescence signal from the spectrograph output was focused to the input slit of the streak camera. Both spectrally and temporally resolved fluorescence signal was obtained at a single shot which was averaged over multiple excitation shots for better S/N ratio. The temporal resolution of the instrument was measured to be ~15 ps at 25 ps/mm sweep speed.

Quantum chemical calculations were performed using GAMESS software package employing density functional theory (DFT) method using B3LYP functional and 6-311 G (d,p) basis set.[32-34]

## Results and Discussion

### Steady state study

Figure 1A shows the absorption spectra of the dyads I and II in toluene. Absorption spectra of the corresponding sub-units III and IV in the same solvent have been shown in Figure 1B. In each case, strong absorption band appearing in the 380 – 460 nm region is assigned to the Soret band and the well-resolved vibronic band appearing in the 500-700 nm region to the Q-band absorption. It is important to note that both the Soret and the Q absorption bands of $N_2S_2$are red shifted as compared to those of $ZnN_4$. This suggests that the energy levels of both the $S_2$ and $S_1$states of $N_2S_2$are lower as compared to those of the corresponding levels of $ZnN_4$.

Figure 1B also shows that the absorption spectrum calculated by addition of those of III and IV agrees well with those of two dyads. This clearly suggests that the absorption characteristics of both the sub-units III and IV are not significantly altered by integrating them in the dyads and hence indicates very weak

electronic interaction between the two subunits as well as with the linker in the ground state of each of these two dyads.

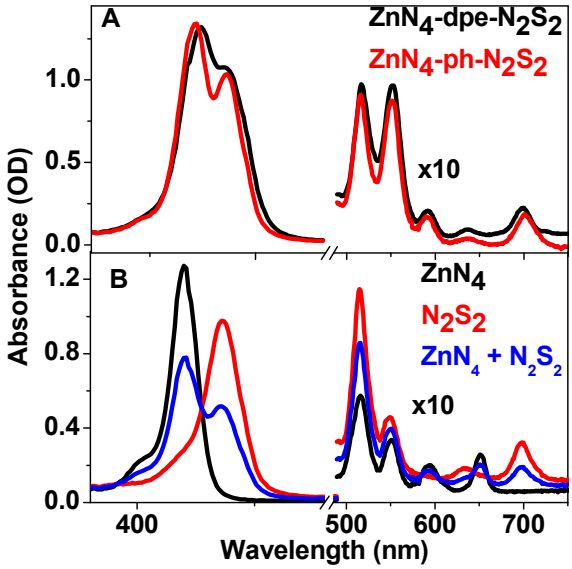


Fig. 1 Steady state absorption spectra of two dyads (A) and the constituent sub-units (B).

Emission spectra of the dyads I and II have been shown in Figures 2A and 2B, respectively. For each of these two dyads, emission spectrum recorded using 415 nm photoexcitation consists of dual emission bands. Relatively weaker one, appearing in the 470 – 670 nm region, consists of two vibronic bands, which are the characteristics of the fluorescence emission originating from the $S_1$ state of the sub-unit $ZnN_4$ (III) (not shown in Figure 2, vide infra). The more intense emission band appearing in the 670 – 850 nm region with the maximum at ca 720 nm is the characteristic of the sub-unit $N_2S_2$ (IV). However, on photoexcitation at 440 nm, which selectively excites the sub-unit $N_2S_2$, the intensity of the emission from the sub-unit $ZnN_4$ reduces significantly. The fact that, in spite of 415 nm photoexcitation, which selectively excites the $ZnN_4$ unit, more intense emission has been observed from the $N_2S_2$unit which suggests efficient transfer of energy from the $S_1$ state localized on the $ZnN_4$ unit to that of the $N_2S_2$ unit in the dyad. The fluorescence spectra are measured to be independent of concentration (in the range of 10 to 50 μM) and suggest that the observed energy transfer process is of intramolecular in nature. In the case of dyad II, in which two sub-units are linked by a phenyl group, contribution of the emission from the $ZnN_4$ unit is negligibly small and hence suggests very fast and near quantitative transfer of energy from the sub-unit $ZnN_4$to the sub-unit $N_2S_2$. In the case of dyad I, in which the diphenylethyne group is the linker, the emission spectrum recorded following 415 nm photoexcitation has a small contribution from the $ZnN_4$ unit and the energy transfer efficiency in this case has been determined to be close to 90%. Thus, steady state studies clearly indicate efficient energy transfer from the $ZnN_4$ unit to the $N_2S_2$ unit in the cases of both the dyads. However, it is noted that exclusive excitation to one unit is not possible and thus energy transfer efficiency calculation from steady state measurement is approximate one. We like to mention that the energy transfer rate has been directly measured from time resolved studies and energy transfer efficiencies were determined using experimental energy transfer rates using equation (1).

**Time resolved fluorescence studies**

To investigate the rates and efficiencies of the energy transfer process from the $ZnN_4$to the $N_2S_2$ moiety, we adopted the streak camera based fluorescence spectroscopic technique having about 15 ps time resolution. Time evolution of the transient fluorescence spectra and temporal evolution of the

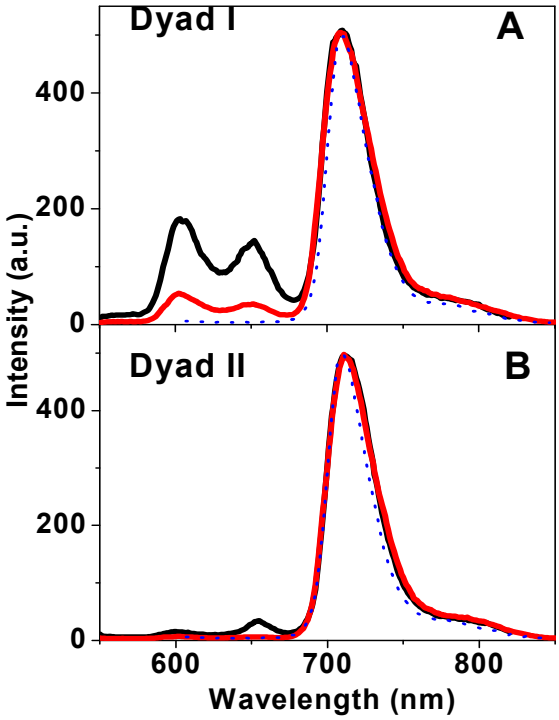


Fig. 2 Fluorescence spectra of Dyad I (A) and Dyad II(B) in toluene on photoexcitation using 415 nm (black line) and 440 nm (red line) light. Dotted blue line shows the fluorescence spectra of monomeric $N_2S_2$ unit.

emission intensity monitored at 620 and 720 nm in the case of the Dyad I following photo-excitation at 400 nm are shown in Figure 3. At 400 nm, we could selectively excite the $ZnN_4$ unit (see Figure 1B) to the $S_2$ state, which quickly relaxes to the $S_1$ state via internal conversion and energy transfer to the $N_2S_2$ unit takes place from the $S_1$ state of the donor unit. Thus, energy transfer dynamics could be accurately monitored, even if a small fraction of these dyads is directly excited to the $S_2$ state, in which the energy is localized at the $N_2S_2$ unit. The time-resolved emission spectrum (TRES) recorded within the instrument response time (i.e. at 0 ps delay time following photoexcitation) consists of two emission bands with the maxima at 620 nm and 720 nm. With increase in delay time,

intensity of the 620 nm band decays and that of the 720 nm band rises concomitantly and analyses of the temporal fluorescence profiles monitored at these two wavelengths reveal that the decay and rise times of the emission intensities, respectively, are nearly equal (16.5 ± 0.5 ps). This suggests that evolution of the TRES presented in Figure 3 is associated with the process of energy transfer from the $ZnN_4$ moiety (emission maximum at 620 nm) to the $N_2S_2$ moiety (emission maximum at 715 nm). Appearance of significant emission intensity at720 nm even at zero delay time is obviously due to direct excitation of $N_2S_2$ unit at 400 nm photoexcitation as well as limited temporal resolution of the streak camera (~15 ps). Therefore, significant amount of energy transfer takes place within the time window of the instrument response time. However, we could determine the rate of energy transfer from the $ZnN_4$ to $N_2S_2$ unit from the TRES and temporal kinetics.

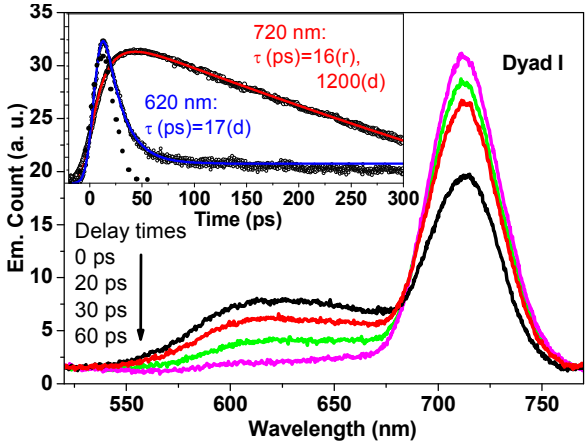


Fig. 3 Time resolved fluorescence spectra of Dyad I in toluene recorded by streak camera. Inset: Temporal profiles (dots) along with the double exponential fit functions (lines) Dotted curve in the inset represents the instrument response function.

The temporal emission profile recorded at 620 nm shows a single exponential decay with the lifetime of 17 ps, followed by another long-lived component, the lifetime of which could not be determined with significant accuracy because of very low intensity as well as the limitation of the streak camera detection recording up to only 1.5 ns. This long-lived emission may be assigned to that from $ZnN_4$ monomer remains as impurity,[19] or from the $ZnN_4$ moiety of that dyad I molecules which do not have geometrical configurations favourable for energy transfer (vide infra).[31]The transient profile recorded at 720 nm shows the rise of emission intensity with the lifetime of 16 ps followed by a slow decay of the emission intensity with the lifetime of about 1.2 ns, which agrees well with the $S_1$ state lifetime of the $N_2S_2$ molecule reported earlier.[25] Thus we determine the energy transfer rate in the case of Dyad I as $k_{ET}(I) = (16.5ps)^{-1} = 6.06 \times 10^{10}\ s^{-1}$ and using equation 1and the value of $k_f(I) = (2.4\ ns)^{-1} = 0.04 \times 10^{10}\ s^{-1}$, the efficiency of the energy transfer process calculated in the case of Dyad I, $\xi_{ET}(I)$, is 0.98.

$$\xi_{ET} = \frac{k_{ET}}{k_{ET} + k_f} \qquad (1)$$

We also recorded the TRES and the temporal profiles at 620and 720nm using streak camera in the case of Dyad II in toluene. We observe that features of time evolution of the TRES are very similar to that observed in the case of Dyad I, but the time domain, in which the evolution of the TRES takes place, is much longer. The temporal profile recorded at 620nm reveals the instrument response time limited rise followed by two exponential decay. The faster decay component has a lifetime of 60ps, but the lifetime of the longer lived component could not be determined accurately because of very small amplitude. Appearance of this component with smaller amplitude suggests near complete energy transfer from the $ZnN_4$ moiety to the $N_2S_2$ moiety. The rise of emission intensity at 720nm with the lifetime of 60 ps also ensures the occurrence of the energy transfer process and the rate of this process has been calculated to be $k_{ET}(II) = 1.67 \times 10^{10}\ s^{-1}$.The efficiency of the energy transfer process $\xi_{ET}(II)$ calculated using equation 1, is about 0.96.

**Transient absorption studies**

Sub-ps time-resolved transient absorption spectroscopic technique, which has better time resolution than that of the streak camera based technique used here, has also been used to study the energy transfer dynamics in the excited states of the dyads. Time evolution of the differential transient absorption spectra recorded following photoexcitation of the Dyad I in toluene using 400 nm laser pulses are shown in Figure 4. We mentioned earlier that 400 nm photons preferentially excite the $ZnN_4$ moiety. Differential transient absorption spectra consist mainly of several intense excited state absorption (ESA) (positive absorbance) bands throughout the wavelength region (470 – 750 nm), overlapped with two weak bands with negative absorbance at 530 and 710 nm. Appearance of well resolved band structures in the differential transient absorption spectra may be attributed to the multiple Q bands in the 500 – 750 nm region (Figures 1A) and strong emission bands at 710 nm (Figures 2A).

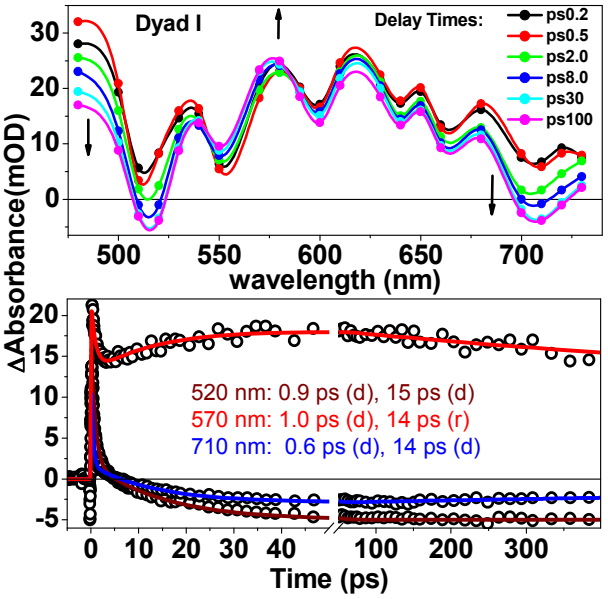


Fig. 4 Time evolution of the transient absorption spectra and temporal profiles recorded a few selective wavelengths following photoexcitation of Dyad I in toluene using 400 nm laser pulses.

Appearance of two near isosbestic points at ca 530 and 570 nm suggests that the process of transformation of one excited species to another must be associated with the evolution of the transient spectra. In conjunction with our time resolved fluorescence data, we infer that decrease in absorbance in the 470 – 530 and 570 – 770 nm regions are associated with the decay of the $S_1$ state, in which the energy is localized at the $ZnN_4$ moiety, whereas the rise of absorption in the 530 – 570 nm represents the energy transfer process from the $ZnN_4$ moiety to the $N_2S_2$ moiety. Therefore, the negative absorbance band appearing at 530 nm is assigned to bleaching and that at 710 nm is to the stimulated emission (SE) from the excited state of the dyad, in which the excitation energy is localized at the $N_2S_2$ moiety.

Temporal profiles of the transient absorption signals recorded at three selective wavelengths along with the multi-exponential fit functions have also been presented in Figure 4. Each of them could be fitted well with a three exponential function having the components with very similar lifetimes. This suggests that each of the transient absorption spectra recorded in the entire 470 – 770 nm region has contributions from both the excited states, in which the singlet state energy is localized either at $ZnN_4$ or $N_2S_2$. The temporal profile recorded at 520 nm is associated with an instrument response time-limited rise of ESA followed by an ultrafast decay of ESA with the lifetime of 0.9 ps leading to the bleaching signal, which subsequently rises slowly with the lifetime of 15 ps. The bleaching signal is long-lived (lifetime is longer than 500 ps). The temporal profile recorded at 710 nm shows the instrument response time-limited rise of ESA, followed by its double exponential decay with the lifetimes of 0.6 and 14 ps leading to a long-lived negative absorbance signal, which may be assigned to stimulated emission from the $N_2S_2$ moiety. Transient signal monitored at 570 nm also shows the instrument response time-limited rise of ESA, which initially decays with about 1.0 ps lifetime but subsequently rises with the lifetime of about 14 ps.

Ultrafast decay of ESA with the average lifetime of about 0.9 ± 0.2 ps, which is associated with each of three transient absorption signals, may be assigned to the $S_2$ state, corresponding to the Soret band. This state is initially populated by absorption of 400 nm light and decays to populate the $S_1$ state, in which the excitation energy remains stored at the $ZnN_4$ moiety, via the internal conversion process. Rise of stimulated emission intensity monitored at 710 nm or the rise of ESA at 520 nm with the lifetime of 14 ps is ascribed to the population of the $S_1$ state of the dyad, in which the excitation energy is localized at the $N_2S_2$ moiety, via energy transfer process. These results and the rate of energy transfer thus calculated ($k_{ET}$ = 14.5 $ps^{-1}$ = 6.9 x $10^{10}$ $s^{-1}$) are in perfect agreement with those obtained in the time-resolved fluorescence experiment.

In the case of dyad II, time evolution of the transient spectra and the temporal profiles recorded at a few selective wavelengths have been presented in Figure 5 and seen to be similar to that of Dyad I. Following the arguments presented above, the ultrafast decay lifetime of ESA (1.2 ± 0.4 ps) is correlated with the internal conversion of the $S_2$ state to the $S_1$ state of the dyad in which the excitation energy remains localized at the $ZnN_4$ moiety. In addition, the rate of energy transfer from the $ZnN_4$ moiety to the $N_2S_2$ moiety ($k_{ET}$ = 60 $ps^{-1}$ = 1.7 x $10^{10}$ $s^{-1}$) in the case of Dyad II could be determined from the rise time of the ground state bleach monitored at 520 nm, SE at 710 nm or ESA at 570 nm.

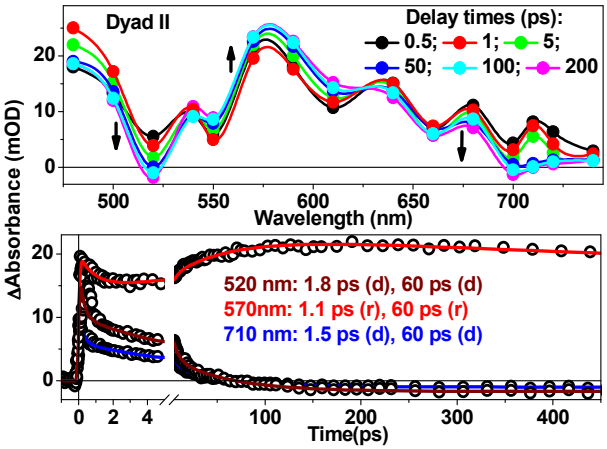


**Fig. 5.** Time evolution of the transient absorption spectra and temporal profiles recorded a few selective wavelengths following photoexcitation of the Dyad II in toluene using 400 nm laser pulses.

**Mechanism of energy transfer**

Time-resolved transient absorption and fluorescence spectroscopic studies presented in the earlier sections reveal that the rate of energy transfer in the case of Dyad II is about four times slower than that in the case of Dyad I. Since both the dyads have the same donor and acceptor moieties, this difference in the energy transfer rates obviously can be attributed to the differences in the characteristics of the spacers connecting them. While the structures of the spacers in these two dyads are very similar, the faster energy transfer rate in the case of Dyad I can be assigned to the smaller distance between the donor and the acceptor.

We compare the energy transfer rates determined for these dyads ($N_2S_2$ substituted dyads) in this work with those already reported for two $N_4$ substituted dyads, in which the donor ($ZnN_4$) and the spacers are same.[15,16] We find that the energy transfer rates in the $N_2S_2$ substituted dyads are nearly four times (for *ph* linked) and 2.5 times (for *dpe* linked) slower as compared to the corresponding $N_4$ substituted dyads. Therefore, although the $N_2S_2$ substituted dyads provide better energy gradient for energy flow due to lower energy of the $S_1$ electronic state of $N_2S_2$, energy transfer process in the hetero-porphyrin system is less efficient as compared to that in the $N_4$ analogue. A series of papers published by Lindsey and coworkers establish the fact that frontier orbital compositions of the energy donor and acceptor porphyrin units greatly influence the through-bond energy transfer dynamics[12-15]. In the case of $ZnN_4$, $a_{2u}$ orbital acts as HOMO, possessing high electron density at the meso position and low electron density at the β position.[13] Thus, in the meso-substituted $ZnN_4$-$N_4$ dyad, the energy transfer rate is found to be remarkably faster than the β–linked dyad due to stronger through-bond electronic interaction in the meso-linked derivative.

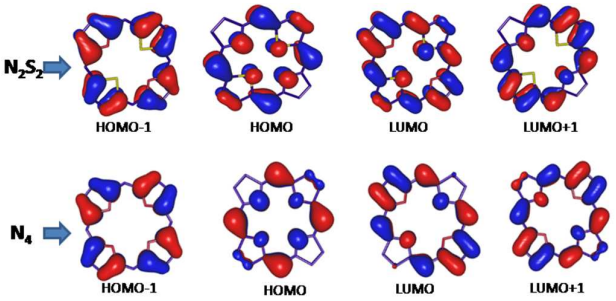


**Fig. 6**. Frontier molecular orbitals of the $N_4$ and $N_2S_2$porphyrins, which influence energy transfer dynamics. Hydrogen atoms are omitted in the figures.

In contrast, pentafluoro substitution at the four phenyl rings of $ZnN_4$ unit, reversal of orbital ordering occur leading to reversal in the energy transfer rate in the meso- and β-linked dyads.[14] In the present study, the donor unit and the linker position for both the dyads are same as *Lindsey's dyads*, whereas the acceptor unit is different, and thus any difference in electronic interaction may originate from the acceptor site. Hence, it is necessary to know the effect of core modification by sulphur substitution on the frontier orbital characteristics, which participate in the electronic interaction and may significantly alter the energy transfer rate. Figure 6 shows the DFT calculated frontier molecular orbitals of porphyrin ($N_4$) and dithiaporphyrin ($N_2S_2$). It is apparent from the frontier orbital pictures that both of the $N_4$ and $N_2S_2$ porphyrins have nearly similar orbital characteristics, which suggest that core modification upon sulphur substitution does not influence the HOMO-LUMO composition. This clearly indicates that through-bond electronic interaction is essentially similar in the $N_4$ and $N_2S_2$ systems. Thus, in comparison to $N_4$-porphyrin, $N_2S_2$-porphyrin is not expected to influence the energy transfer dynamics via electronic interaction.

Numerous studies on intramolecularly connected energy donor and acceptor systems, reveal that the electronic coupling for the energy transfer process follows one or more of three possible mechanisms: a) Förster mechanism by dipole - dipole resonant (Coulombic) or through-space interaction, which is active at longer distances up to 100 Å,[35] b) Dexter mechanism by electron exchange interaction, which requires an orbital overlap and is active at distances less than 10 Å,[36] and c) the super-exchange electronic coupling between the donor, bridge and the acceptor.[37] In the first two cases, the bridge is considered as an inert spacer. The super exchange coupling is believed to decay exponentially with the distance (vide infra).

For the energy transfer process by Förster mechanism, along with other factors, the rate of energy transfer is dependent upon the degree of overlap between the donor emission and the acceptor absorption spectra. The spectral overlap integral for resonance interaction, $J_F$ (in $M^{-1}$ $cm^3$), is determined by equation (2).

$$J_F = \frac{\int F(\upsilon)\varepsilon(\upsilon)\upsilon^{-4}d\upsilon}{\int F(\upsilon)d\upsilon} \qquad (2)$$

The rate of energy transfer (in $s^{-1}$) by Förster mechanism can be calculated using equation (3)

$$k_F = \frac{9000ln10k^2\Phi_D J_F}{128\pi^5 N_A n^4 \tau_D {r_{cc}}^6} \qquad (3)$$

Where, $\Phi_D$ and $\tau_D$ are the fluorescence quantum yield and the lifetime of the donor alone, 'n' is the refractive index of the solvent and $r_{cc}$ is the donor - acceptor center-to-center distance. On the other hand, the Dexter-type energy transfer rate,$k_D$, is given by equation (4),

$$k_D = \frac{2\pi}{\hbar}V^2 J_D \qquad (4)$$

$$J_D = \frac{\int F(\upsilon)\varepsilon(\upsilon)d\upsilon}{\int F(\upsilon)d\upsilon \int \varepsilon(\upsilon)d\upsilon} \qquad (5)$$

where, $J_D$ (in cm) is the exchange overlap integral and can be calculated using equation (5) and 'V' is the electronic coupling matrix element.

**Table 1:** Comparison of the rates and efficiencies of energy transfer processes in $ZnN_4$-$N_4$ and $ZnN_4$- $N_2S_2$ dyads.

| Dyad | $\xi_{ET}$ | $k_{ET}$, $10^{10}$ $s^{-1}$ | $J_F$, $10^{-14}$ $cm^3M^{-1}$ | Förster Rate $10^9$ $s^{-1}$ | Ratio, $J_F^a/J_F^b$ | $J_D$ $10^{-4}$cm | Ratio, $J_D^a/J_D^b$ | $\chi_{TS}$ | $\chi_{TB}$ | Ratio, $k_{ET}^a/k_{ET}^b$ |
|---|---|---|---|---|---|---|---|---|---|---|
| $ZnN_4$-ph-$N_4$[a] | 0.99 | 28 | 6.8 | 29 | 3.8 | 4.35 | 2.2 | 0.10 | 0.90 | 4.5 |
| $ZnN_4$-ph-$N_2S_2$[b] | 0.99 | 6.2 | 1.8 | 8.6 | | 1.95 | | 0.13 | 0.87 | |
| $ZnN_4$-dpe-$N_4$[a] | 0.98 | 4.2 | 6.8 | 2.4 | | 4.35 | | 0.05 | 0.95 | 2.5 |
| $ZnN_4$-dpe-$N_2S_2$[b] | 0.96 | 1.7 | 1.8 | 0.7 | | 1.95 | | 0.04 | 0.96 | |

[a]Ref 13, 15;[b]This work.

Thus, the overlap between the donor emission and acceptor absorption spectra is an important parameter in both Förster and Dexter mechanism because the values of both the resonance integral and the exchange integral depend on the magnitude of the overlap integral. The donor emission and acceptor absorption spectra are shown in Figure 7 and the calculated values of the resonance integral and exchange integral are shown in the insets of the figure.

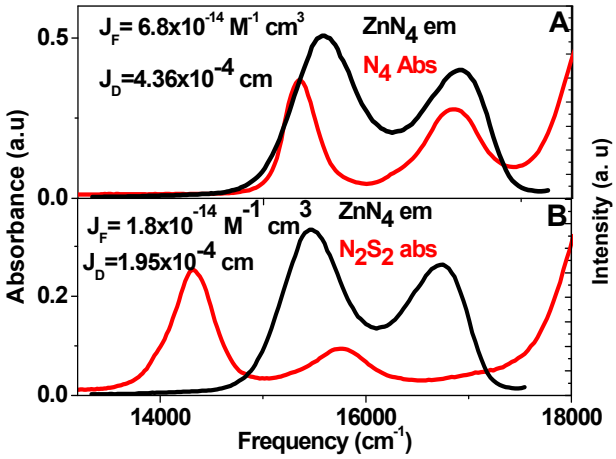


**Fig. 7**. Comparison of the overlap of the $ZnN_4$ emission spectrum with the absorption spectra of $N_4$ (A) and $N_2S_2$ (B). The calculated values of the resonance integral ($J_F$, $M^{-1}cm^3$) and exchange integral ($J_D$, cm) are given in the insets.

Considering the Förster energy transfer mechanism and thus, employing equation (2) and (3), the energy transfer rates in the cases of Dyad I and Dyad II have been calculated to be 8.6 x $10^9$ $s^{-1}$ and6.5 x $10^8$ $s^{-1}$, respectively. Following values were used for calculation of the Förster energy transfer rates: $\Phi_f$ ($ZnN_4$) = 0.03, $\tau$($ZnN_4$) = 2.4 ns, n(toluene) = 1.49, r = 13Å (*dyad* I) and 20Å (*dyad* II), $k^2$ = 0.84 (a dynamic average of different conformations is assumed due to the fact that the donor and acceptor units can freely rotate around the single bonds).[38] These calculated rates are significantly smaller than the experimentally determined rates of energy transfer, which clearly suggests that dipole-dipole resonance mechanism does not control the energy transfer rate in these dyad systems. Indeed, the dipole-dipole mediated through space contribution ($\chi_{TS}$) to experimentally measured energy transfer rate is around 4% and 13% for dyad I and dyad II, respectively, whereas, through bond contribution ($\chi_{TB}$) to energy transfer process dominates in both the dyads (Table 1).This is in accordance with the energy transfer mechanism observed in numerous meso-meso linked porphryrin dyad assemblies.[12-17]It may be noted that the ratios of the experimentally determined rates to those calculated assuming Förster mechanismin the *dpe* linked dyad) are significantly larger (about 10 - 14 times) as compared to those in the case of *ph* linked dyads (about 4 - 6 times).

On the other hand, the Dexter mechanism via exchange interaction generally dominates when the donor and acceptor orbitals are in close proximity (within a few Å). In *dpe* and *ph* linked porphyrin dyads, centre-to-centre distance is ~20Å and ~13Å, respectively. Thus direct orbital overlap between the donor and acceptor units is expected to be too weak to impart Dexter exchange mediated energy transfer. An alternative mechanism is the bridge mediated through-bond super-exchange interaction, which can provide necessary electronic coupling for Dexter energy transfer to become feasible. Indeed, through-bond electronic interaction has been established to be the dominant energy transfer pathway in porphyrin dyads with various linker groups.[12-14]

In the case of either Dexter exchange mechanism or through-bond super-exchange mechanism, rate of energy transfer should be proportional to the value of the exchange integral ($J_D$ in equation 5), provided the electronic interaction is comparable and the later governs the electronic coupling matrix element. The DFT calculated molecular orbital composition (Figure 6) clearly suggests that orbital contribution at the meso position of the $N_4$ and $N_2S_2$ acceptors are similar. Hence it is reasonable to assume that the electronic coupling matrix element, V, is similar in magnitude for both the $N_4$ and $N_2S_2$ acceptor containing dyads. In this situation, rate of energy transfer is expected to be proportional to $J_D$. Indeed, the ratio of the values of $J_D$ of $ZnN_4$-$N_4$ pair to that of $ZnN_4$-$N_2S_2$ pair closely corresponds to the ratio of the energy transfer rates observed in the case of the *dpe* linked dyads (Table 1). This essentially confirms that energy transfer rate in the Dyad II is controlled by through-bond super-exchange mechanism.

We calculated the magnitude of electronic coupling (V) from the experimentally determined values of the energy transfer rates and the exchange integrals using equation (4). For dyad II, the value of V is calculated to be 8.58 $cm^{-1}$.The magnitude of this parameter indicates a moderate coupling between the donor and acceptor components, retaining their electronic identity in the dyad form. This is in agreement with the steady state spectroscopic results discussed in section 3.1. For dyad I, the value of V is calculated to be 17.5 $cm^{-1}$. The enhanced value of V in dyad I is due to the shorter distance between the donor and the acceptor groups as compared to that in Dyad II. The value of the attenuation factor (β) has been calculated to be 0.178 $Å^{-1}$ using equation 6.

$$V = V_0 \exp\left(-\frac{\beta}{2} r_{cc}\right) \qquad (6)$$

The value of β ~0.2 is typical for the phenylethyene bridge mediated energy transfer process.[38] Hence, the calculation

presented above is valid for the super-exchange mediated energy transfer mechanism operative in both the dyads.

However, unlike in the case of the *dpe* - linked dyads, in the case of the *ph* - linked dyads, the energy transfer mechanism appears to be more complicated when we compare the energy transfer rate determined in this work with that previously reported for a $N_4$ substituted dyad. The ratio of the rate of the energy transfer process determined for the $N_4$-substituted phenyl-linked dyad to that of the $N_2S_2$ – substituted one (i.e. $k_{ET}^{a}/k_{ET}^{b}$ = 4.5) is higher than the ratio of the calculated values of the exchange integrals (i.e. $J_D^{a}/J_D^{b}$ = 2.2). This suggests that the contribution of the energy transfer process occurring via through-bond mechanism is not the major one in these dyads, unlike in the case of the *dpe* - linked dyads. In exchange mediated energy transfer, the difference between the energies of the excited state of the donor and the bridge ($\Delta E_{DB}$) plays an important role. An inverse square dependence of the energy transfer rate on $\Delta E_{DB}$ was theoretically predicted and experimentally verified too.[38] Exchange mediated energy transfer in the case of Dyad I is expected to be of lesser importance as $\Delta E_{DB}$ in the case of the *ph* - bridge is much larger than that of the *dpe*-bridge. On the other hand, purely dipole - dipole mediated Förster resonance energy transfer mechanism cannot account for the measured energy transfer rate, which is about seven times faster than the calculated one (vide supra). Surprisingly, we find that ratio of the rates of the energy transfer processes in the *ph* - linked dyads is close to the ratio of the resonance integral ($J_F$) (Table 1). This possibly suggests that resonance interaction via multipole states may contribute to the energy transfer mechanism. Previous studies have shown that at short distances, corrections due to multipole contribution to the dipole-dipole approximation may increase the energy transfer rate by a factor of five or more.[39] In the *ph* - linked porphyrin dyads, the center-to-center distance between the energy donor and acceptor units is ~13Å, which is sufficiently short to impart such effect. It is also reported by Lindsey et. al. that the effect of orbital ordering reversal on energy transfer rate in the *ph* - linked dyad is less prominent as compared to that of the *dpe* - linked dyads.[15] This led them to infer that the through-bond mechanism becomes less important in the case of the *ph* - linked dyad as compared to that of the *dpe*- linked dyads. The observed rate dependence with linker length or donor / acceptor character could not be fully accounted either by pure through-space or through-bond mechanism. A role over from through-bond to through-space mechanism is hinted in previous studies by Lindsey and coworkers.[15] Our present observation is also suggestive of similar intriguing mechanistic involvement and warrants further studies to understand the through-space versus through-bond energy transfer mechanism in covalently linked porphyrin dyads.[40]

## Conclusions

We have studied the energy transfer dynamics in two molecular dyads, in which zinc porphyrin and dithiaporphyrin subunits are covalently linked by two different molecular bridges, in toluene using ultrafast transient absorption and fluorescence spectroscopic techniques. Experimental results reveal that core modification of the acceptor porphyrin by two sulphur atoms leads to reduction in the rate of energy transfer, although the efficiency of energy transfer is not significantly affected. Similar to the covalently linked homoporphyrin assembly, contribution of the energy transfer process via Förster mechanism to the total rate is less nearly by one order of magnitude and the energy transfer dynamics in *dpe* - linked dyad is mainly governed by Dexter exchange mechanism. The significant retardation in energy transfer rates in dithiaporphyrin ($N_2S_2$) based dyads can be quantitatively attributed to the decrease in exchange integral between the $ZnN_4$ donor and $N_2S_2$ acceptor. In *ph* - linked dyads, multipole mediated resonance interaction plays dominant role in the energy transfer dynamics possibly due to shorter distance between the donor and acceptor units. In both the dyads, the electronic factor which plays crucial role in energy transfer rate of covalently linked porphyrin assemblies is not influenced by sulphur substitution at the core of porphyrin. This has been apparent from the comparison of DFT calculated HOMO-LUMO characteristics of porphyrin and dithiaporphyrin. Thus, core modified porphyrins, though provide better gradient for energy flow in multiporphyrin antenna assembly, the decrease in spectral overlap integral significantly reduce the rate of energy flow which may be detrimental to the energy harvesting efficiency.

## Notes and references

1 A. K. Burrell, D. L. Officer, P. G. Plieger, D. C. W. Reid, *Chem. Rev.* 2001, **101**, 2751.
2 D. Gust, T. A. Moore, A. L. Moore, *Acc. Chem. Res.* 1993, **26**, 198.
3 V. Balzani, S. Campagna, G. Denti, A. Juris, S. Serroni, M. Venturi, *Acc. Chem. Res.* 1998, **31**, 26.
4 D. Kim, A. Osuka, *Acc. Chem. Res.* 2004, **37**, 735.
5 Y. Nakamura, N. Aratani, A. Osuka, *Chem. Soc. Rev.* 2007, *36*, 831.
6 S. Prathapan, T. E. Johnson, J. S. Lindsey, *J. Am. Chem. Soc.* 1993, **115**, 7519-7520.
7 R. W. Wagner, J. S. Lindsey, *J. Am. Chem. Soc.*1994, **116**, 9759.
8 R. W. Wagner, J. S. Lindsey, J. Seth, V. Palaniappan, D. F. Bocian, *J. Am. Chem. Soc.* 1996, **118**, 3996-3997.
9 A. A. Bothner-By, J. Dadok, T. E. Johnson, J. S. Lindsey, *J. Phys. Chem.*1996, **100**, 17551.
10 J. Seth, V. Palaniappan, T. E. Johnson, S. Prathapan, J. S. Lindsey, D. F. Bocian, *J. Am. Chem. Soc.* 1994, **116**, 10578.
11 A. Osuka, N. Tanabe, S. Kawabata, I. Yamazaki, Y. Nishimura, *J. Org. Chem.* 1995, **60**, 7177.
12 D. Holten, D. F. Bocian, J. S. Lindsey, *Acc. Chem. Res.* 2002, **35**, 57.

13 J. P. Strachan, S. Gentemann, J. Seth, W. A. Kalsbeck, J. S. Lindsey, D. Holten, D. F. Bocian, *J. Am. Chem. Soc.*1997, **119**, 11191.
14 S. I. Yang, J. Seth, T. Balasubramanian, D. Kim, J. S. Lindsey, D. Holten, D. F. Bocian, *J. Am. Chem. Soc.*1999, **121**, 4008.
15 S. I. Yang, R. K. Lammi, J. Seth, J. A. Riggs, T. Arai, D. Kim, D. F. Bocian, D. Holten, J. S. Lindsey, *J. Phys. Chem. B* 1998, **102**, 9426.
16 F. Li, S. W. A. Gentemann, J. Seth, J. S. Lindsey, D. Holten, D. F. Bocian, *J. Mater. Chem.*1997, **7**, 1245.
17 P. Hascoat, S. I. Yang, R. K. Lammi, J. Alley, D. F. Bocian, J. S. Lindsey, D. Holten, *Inorg. Chem.* 1999, **38**, 4849.
18 J. Otsuki, Y. Kanazawa, A. Kaito, D.-M. S. Islam, Y. Araki, O. Ito, *Chem. Euro. J.* 2008, **14**, 3776.
19 B. Ventura, F. Barigelletti, F. Lodato, D. L. Officer, L. Flamigni, *Phys. Chem. Chem. Phys.* 2009, **11**, 2166.
20 M. J. Broadhurst, R. Grigg, A. W. Johnson, *J. Chem. Soc. D* 1969, 1480.
21 M. J. Broadhurst, R. Grigg, A. W. Johnson, *J. Chem. Soc. C* 1971, 3681.
22 R.P. Pandian, D. Reddy, N. Chidambaram, T. K. Chandrashekar, *Proc. Indian Acad. Sci.(Chem. Sci.)*1990, **102**, 307.
23 A. Srinivasan, B. Sridevi, M. V. Reddy, S. J. Narayanan, T. K. Chandrashekar, *TetrahedronLett.* 1997, **38**, 4149.
24 A. Ulman, J. Manassen, F. Frolow, D. Rabinovich, *Inorg. Chem.*1981, **20**, 1987.
25 M. Yedukondalu, M. Ravikanth, *Coord. Chem. Rev.* 2011, **255**, 547.
26 I. Gupta, M. Ravikanth, *Coord. Chem. Rev*. 2006, **250,** 468-518.
27 S. Rai, M. Ravikanth, *J. Org. Chem.* 2008, **73**, 8364.
28 M. Yedukondalu, M. Ravikanth *J. Porphyrins Phthalocyanines*. 2011, **15**, 83.
29 S. Punidha, S. Rai, M. Ravikanth, *J. Porphyrins Phthalocyanines*, 2008, **12**, 1030.
30 S. Rai, M. Ravikanth, *Tetrahedron*2007, *63*, 2455.
31 J. A. Mondal, G. Ramakrishna, A. K. Singh, H. N. Ghosh, M. Mariappan, B. G. Maiya, T. Mukherjee, D. K. Palit, *J. Phys. Chem.*2004, **108**, 7843.
32 A. D. Becke, *J. Chem. Phys.*1993, **98**, 5648.
33 C. Lee, W. Yang, R. G. Parr *Phys. Rev. B* 1998, **37**, 785.
34 M. W. Schmidt, K. K. *Baldridg*e, J. A. Boatz, S. T. Elbert, M. S. Gord*onJ. H. Jens*en, S. Koseki, N. Matsunaga, K. A. Nguyen, S. J. Su, T. L. Windus, M. Dupuis, J. A. Montgomery, *J. Comput. Chem.* 1993, **14**, 1347.
35 (a)T. Förster, *Naturwissenschaften*1946, **33**, 166. (b)T. Förster, *Ann. Phys.* 1948, **2**, 55.
36 L. Dexter, *J. Chem. Phys.*1953, **21**, 836.
37 H. M. McConnell, *J. Chem. Phys,* 1961, **35**, 508.
38 K. Pettersson, A. Kyrychenko, E. Ronnow, T. Ljungdahl, J. Martensson, B. Albinsson, *J. Phys. Chem. A,* 2006, **110**, 310.
39 J. Chang, *J. Chem. Phys.* 1967, **77**, 3901.
40 R. Metivier, F. Nolde, C. Mullen, T. Basche, *Phys. Rev. lett.* 2007, **98**, 047802.

**Graphical Abstract**